Characterization and Photocatalytic Activity of TiO_2(rod)-SiO_2-Polyaniline Nanocomposite

Sri Wahyuni[1,2], Eko Sri Kunarti[2], Respati Tri Swasono[2], and Indriana Kartini[2,*]

[1]*Department of Chemistry, Faculty of Mathematics and Natural Sciences, Universitas Negeri Semarang, Jl. Raya Sekaran-Gunungpati, Semarang 50229, Indonesia*

[2]*Department of Chemistry, Faculty of Mathematics and Natural Sciences, Universitas Gadjah Mada, Sekip Utara, Yogyakarta 55281, Indonesia*

Received February 27, 2017; Accepted January 11, 2018

ABSTRACT

A study of TiO_2(rod)–SiO_2 composites coated with polyaniline (PANI) has been performed. PANI was synthesized through in-situ *polymerization of aniline at various concentration (0.0137, 0.0274, and 0.0411 M) on the composite under acidic condition. PANI was confirmed by the appearance of C=N, C=C vibrations and the redshift of the band-gap from 3.14 eV for the TiO_2(rod)–SiO_2 into 3.0 eV for the TSP01 composite. It is also shown that the polymerization does not change the crystal structure of TiO_2(rod)–SiO_2 as confirmed by the XRD pattern. The TEM image shows a mixed structure of SiO_2 coated by TiO_2(rod)-PANI layers and the oxides coated by PANI layers. Therefore, the surface area of the resulted TiO_2(rod) and the composites did not change significantly. The TiO_2(rod)–SiO_2-PANI composite give small improvement under visible irradiation from 20.25 to 25.59% (around 5% from the bulk of TiO_2(rod)) and from 25.03 to 25.59% (around 2% from TiO_2(rod)-SiO_2 composite). The mixed structure of the composites, as well as the formation of excessive layers of PANI, are possibly the case for the low photoactivity. Further improvement to obtain a core-shell structure with a thin layer of PANI is still sought.*

Keywords: *TiO_2(rod)–SiO_2; composite; PANI; photocatalytic*

ABSTRAK

*Telah dilakukan penelitian terhadap komposit TiO_2(rod)–SiO_2 yang dilapisi dengan polyaniline (PANI). PANI disintesis melalui suatu proses polimerisasi oksidatif anilin '*in situ*' pada beberapa konsentrasi (0,0137, 0,0274, dan 0,0411 M) di permukaan komposit di dalam larutan asam. PANI terkonfirmasi dengan munculnya vibrasi C=N dan C=C dan bergesernya band-gap yaitu 3,14 eV untuk TiO_2(rod) ke daerah sinar tampak yaitu 3,00 untuk TSP01. Pola difraksi XRD menunjukkan bahwa polimerisasi tersebut tidak mengubah struktur anatas dari TiO_2(rod) dalam komposit. Citra TEM menunjukkan bahwa struktur komposit merupakan campuran dari TiO_2(rod)–SiO_2 terlapisi PANI, TiO_2(rod) terlapisi PANI, dan SiO_2 yang terlapisi PANI juga. Analisis luas permukaan menunjukkan perubahan luas area yang kecil dari TiO_2(rod), TiO_2(rod)–SiO_2 dan TSP. TSP01 menunjukkan sedikit peningkatan aktifitas fotokatalitik di bawah radiasi sinar tampak yaitu dari 20,25 sampai 25,59% (sekitar 5% lebih tinggi daripada aktifitas TiO_2(rod)), dan dari 25,03 ke 25,59% (sekitar 2% lebih tinggi dibandingkan aktifitas T TiO_2(rod)–SiO_2). Struktur oksida campuran maupun terbentuknya lapisan PANI berlebih menjadi penyebab rendahnya aktivitas fotokatalitik ini. Penelitian lebih lanjut untuk memperoleh struktur 'core-shell' yang lebih baik dengan lapisan PANI yang lebih tipis sedang direncanakan.*

Kata Kunci: *TiO_2(rod)–SiO_2; komposit; PANI; fotokatalitik*

INTRODUCTION

In recent years, conducting polymer/inorganic hybrid materials have been extensively studied because of their potential applications in chemistry, physics, electronics, optics and biotechnology [1-2]. Conducting polymers have already been widely used in photovoltaic devices such as solar cells, light-emitting diodes, and corrosion-protecting paint [3-4]. The physical and chemical properties of final conducting polymer/inorganic composite can be tailored through proper selection of conducting polymer type and inorganic material for particular purposes. Although there are plenty of conducting polymers, little work has been done on using conducting polymer to modify TiO_2(rod) to decompose organic pollutions. As a typical conducting polymer, PANI has unique electrical, optical and photoelectric properties, and most importantly, it is cheaper than other conducting polymers. Some researchers have investigated the effect of

* Corresponding author.
Email address: indriana@ugm.ac.id

DOI: 10.22146/ijc.22550

incorporation of PANI to the photocatalytic performance of TiO_2 [4-6]. One of the research reported that PANI acts as a sensitizer to the neat TiO_2 by triggering TiO_2 to absorb photon under visible irradiation [6,13]. Compared to the neat TiO_2, the PANI-TiO_2 nanocomposites showed better photocatalytic activity in the photodegradation of methyl orange under sunlight [6]. Another research revealed that the modification of TiO_2 by PANI improved the photocatalytic degradation of phenol due to the synergetic effect of PANI and TiO_2 [4]. PANI modified TiO_2 nanocomposite not only absorbs the UV light but also significantly absorbs the visible and near IR [5]. PANI has a forbidden band gap of 2.8 eV, showing strong absorption in the region of visible light. Hence, it may function as a sensitizer to TiO_2 so PANI modified TiO_2 have better photocatalytic activity than neat TiO_2 [6].

Beside TiO_2-PANI, many studies have been done to explore the properties of TiO_2-SiO_2. It is revealed that addition of SiO_2 to TiO_2 improved some characteristic of pristine TiO_2 like the surface area, the homogeneity, and its absorptivity. The changes of these properties improved the photocatalytic activity of TiO_2 [7]. Silica-modified TiO_2 was also reported to exhibit a better photocatalytic performance than TiO_2 itself [8]. The improved performance came especially from two important things, the interaction between TiO_2 and SiO_2 and improved adsorption of the pollutant on the silica over pure TiO_2. Principally, there are two types of interaction of TiO_2 and SiO_2 that is physical with such weak forces as van der Waals, and chemical with the formation of Ti-O-Si bonds [9]. Depositing TiO_2 on silica develops a new surface characterized by the presence of Lewis and Brønsted acid sites [10]. The degree of interaction depends on the preparation methods and synthesis conditions [11]. In the photocatalytic evaluation of the composites, it is found that the organic pollutant more adsorbed on SiO_2, so the presence of SiO_2 in TiO_2-SiO_2 mixed oxide raised the concentration of pollutant near the TiO_2 sites and finally increased the photocatalytic activity [1,10]. These materials have been considered to be used not only as catalytic supports but also as catalysts through the generation of new catalytic active sites [8,12-13]. It is also well known that silica surface is fairly-unreactive, however, the silica surface hydroxyls generally act as adsorptive/reactive sites because of their hydrophilic character [8].

Most publications reported modification on nanoparticle TiO_2. Recently, lower dimensions of nanostructured TiO_2 attract research interest due to their electronic and optical properties [14-16]. One-dimensional (1-D) TiO_2 nanostructures such as nanowires and nanotubes have been investigated extensively due to their superior electrochemical properties, which are attributed to dimensional anisotropy, and electron transport pathway [14,17]. Therefore, this study proposed to modify nanorod TiO_2 by coating with SiO_2 and PANI. A various concentration of PANI that was formed by in situ chemical oxidative polymerization was studied. Firstly, TiO_2(rod) was synthesized through the solvothermal method as well as spherical SiO_2, then the dispersed TiO_2(rod) was added dropwise to the silica spheres. PANI was introduced to the powder of the TiO_2(rod)–SiO_2 by in situ polymerization at various concentration. The photodegradation of methylene blue under visible light was used to evaluate the photocatalytic performance of the resulted powders.

EXPERIMENTAL SECTION

Materials

Aniline monomer (Merck Company, Germany) was distilled two times under vacuum and stored below 4 °C prior to use. TiO_2(rod), SiO_2 and the TiO_2(rod)–SiO_2 were synthesized using the same method as the previous study [18]. All chemicals including ammonium peroxydisulfate (APS, $(NH_4)_2S_2O_8$), hydrochloric acid (HCl) and methylene-blue, were purchased from Merck as analytical grade and used as received.

Instrumentation

The equipment used in this research include Teflon-lined autoclave, magnetic stirrer, glass equipment, X-ray Diffractometer, TEM, BET surface area analyzer, FT-IR, Diffuse-Reflectance-UV-Vis, and UV-Vis spectrophotometer.

Procedure

Attachment of PANI to form TSP was done by in situ chemical oxidative polymerization of aniline on the TiO_2(rod)–SiO_2 [4-5]. One g of TiO_2(rod)–SiO_2 powder was dispersed into 80 mL of 1.2 M HCl under ultrasonication for 30 min to obtain a uniform suspension. Various quantitative of aniline (0.0137, 0.0274, and 0.0411 M) was added carefully to the solutions after that APS dissolved in 1.2 M HCl [5] with the molar ratio of aniline to APS of 1:1.15 was added to the reaction vessel dropwise under vigorously stirring in the ice-water bath. Then, the mixture was allowed to polymerize until a green precipitate of emeraldine salt of PANI was formed while stirring for 5 h. The reaction mixture was filtered under vacuum and washed with ethanol and water and then dried at 60 °C for 24 h [4-5]. The nanocomposites were labelled TSP01, TSP03, and TSP04, where 01, 03, and 04 refer to the

concentration of aniline during the polymerization process, namely 0.0137, 0.0274, and 0.0411 M, respectively.

Characterizations of TSP composites

The X-ray diffraction (XRD) patterns were performed in the range of 2θ = 10–80° on a Shimadzu-diffractometer, using Cu Kα radiation (λ = 0.15406 nm) as an X-ray source, operated at 40 kV and 30 mA. Crystallite size of anatase TiO_2 can be calculated from the line broadening by Scherer's formula.

Fourier-transform infrared spectra (FT-IR) of the samples were recorded on the spectrometer (Shimadzu) in the range of 400–4000 cm^{-1}. Measurements were performed in the transmission mode in spectroscopic grade KBr pellets for all the powders. A diffuse-reflectance-UV Vis type Shimadzu 2450 was used to obtain the reflectance spectra of the catalysts over a range of 200–800 nm. Transmission electron microscopy (TEM) study was carried out on a JEOL JEM-1400 electron microscope to identify the morphology of TiO_2(rod), TiO_2(rod)–SiO_2, and TSP. The samples of TEM were prepared by dispersing the powder in ethanol; the dispersed samples were then dropped on carbon-coated copper grids. The BET surface area was determined using Surface Area Analyzer (Nova 3200e Quantachrome).

Photocatalytic activity test

The photocatalytic activity of TiO_2(rod), TiO_2(rod)–SiO_2, and TSP nanocomposite were evaluated by determining the degradation of methylene blue as an organic pollutant under visible light. The powder of TiO_2(rod), TiO_2(rod)–SiO_2 or TSP of as much as 50 mg was added to 50 mL of an aqueous solution of methylene blue (10 mg L^{-1}). The suspension was stirred in the dark condition at room temperature (25 °C) for 30 min to achieve adsorption equilibrium for methylene blue. Afterward, the suspension was illuminated by a 100 W Xenon lamp with a UV-filter for 90 min. Samples were then taken out regularly from the reactor and centrifuged immediately for separation of any suspended solid. The concentration of remaining methylene blue was obtained by measuring the absorbance of samples at λ max = 663 nm using a UV-Vis spectrophotometer. The determined absorption was converted to concentration through the standard calibration curve. Since the absorption is linear to the concentration, that the photocatalytic degradation efficiency was calculated using the equation:

$$R\% = \frac{A_0 - A_t}{A_0} x100$$

where R% is degradation efficiency of methylene blue, A_0 the initial absorbance of methylene blue in aqueous solution and A_t the absorbance of methylene blue in aqueous solution at different reaction time, t [19-20].

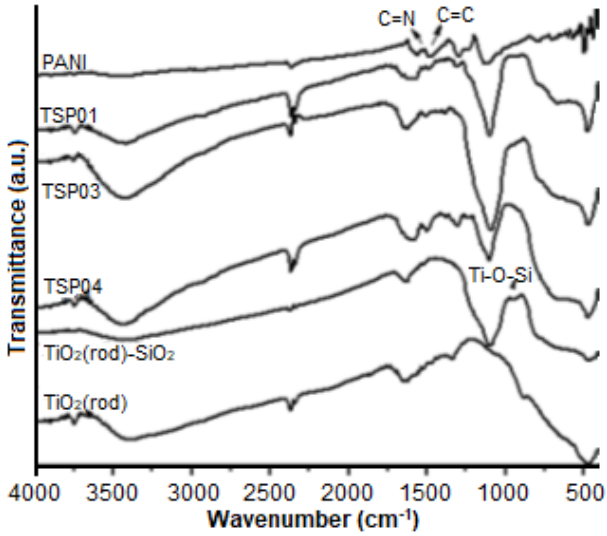

Fig 1. FT-IR spectra of PANI, TiO_2(rod), TiO_2(rod)–SiO_2, and TSP

RESULT AND DISCUSSION

FT–IR Spectra

Fourier transform–infrared (FT–IR) spectroscopy was used to characterize the prepared TSP nanocomposite (TSP01, TSP03, and TSP04). Fig. 1 compares the FT-IR absorption spectra of TiO_2(rod), TiO_2(rod)–SiO_2, TSP composites (TSP01, TSP03, and TSP04), and PANI-HCl. The main characteristic peaks of doped PANI are assigned as follows [4,21]: the band at 3454 cm^{-1} is attributable to N–H stretching mode, C=N and C=C stretching mode for the quinonoid (Q) and benzenoid (B) rings occur at 1587 and 1492 cm^{-1}. The bands at 1290 and 1226 cm^{-1} have been attributed to C–N stretching mode for the benzenoid unit, while the band at 1155 cm^{-1} is assigned to a quinonoid unit of doping PANI [4]. The characteristic peak of TiO_2 at 484 cm^{-1} is so wide that it hides the finger peak in the TSP composite. The peaks at 3441.01 and 1496.76 cm^{-1} corresponding to the N–H stretching vibration and C=C bond, respectively. The initial concentration of aniline in the polymerization solution resulted in PANI layer on TiO_2(rod)–SiO_2 composites [22].

UV–Vis Diffuse Reflectance Spectra

UV–Vis diffuse reflectance spectra of TiO_2(rod), TiO_2(rod)–SiO_2, and TSP composites were shown in Fig. 2. PANI has good absorption in the UV range and especially in the visible light region [4]. Compared to

the TiO_2(rod)–SiO_2, the absorption of TSP sample increased over the whole range of visible light whereas slightly decreased in the UV range. The band gap of TSP, TiO_2(rod)–SiO_2 and TiO_2(rod), obtained from the wavelength values corresponding to the intersection point of the vertical and horizontal parts of the spectra were shown in Table 1. The band-gap was calculated using the equation: $hc/\lambda_{edge} = E_g$, where E_g the band-gap (eV), h was the Planck's constant, c was the light velocity (m/s), and λ_{edge} was the wavelength (nm) [23-24]. It showed that the band gap of the TSP composite was slightly lower than that of TiO_2(rod)–SiO_2 and TiO_2(rod). The TSP composites could produce more electron-hole pairs under visible light illumination, resulting in high photocatalytic activities. By looking at the spectra in Fig. 2, it can be explained that the TSP composite absorbs more light at wavelengths between 400 and 700 nm than the TiO_2(rod)–SiO_2 composite. Neglecting other factors, more visible light absorption should increase the number of electron-hole pairs in the catalyst.

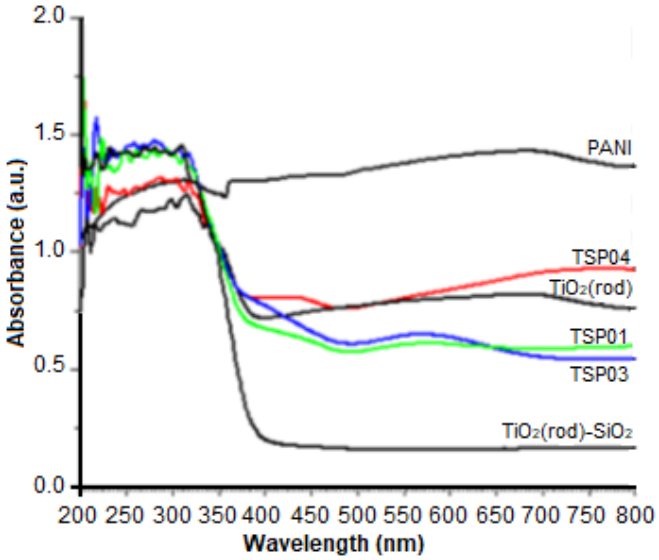

Fig 2. UV–Vis diffuse reflectance spectra of PANI, TiO_2(rod), TiO_2(rod)–SiO_2, and TSP

Table 1. Band-gap of TiO_2(rod), TiO_2(rod)-SiO_2, and TSP

Sample	TiO_2(rod)	TiO_2(rod)–SiO_2	TSP01	TSP03	TSP04
Band-gap (eV)	3.13	3.14	3.00	3.01	3.02

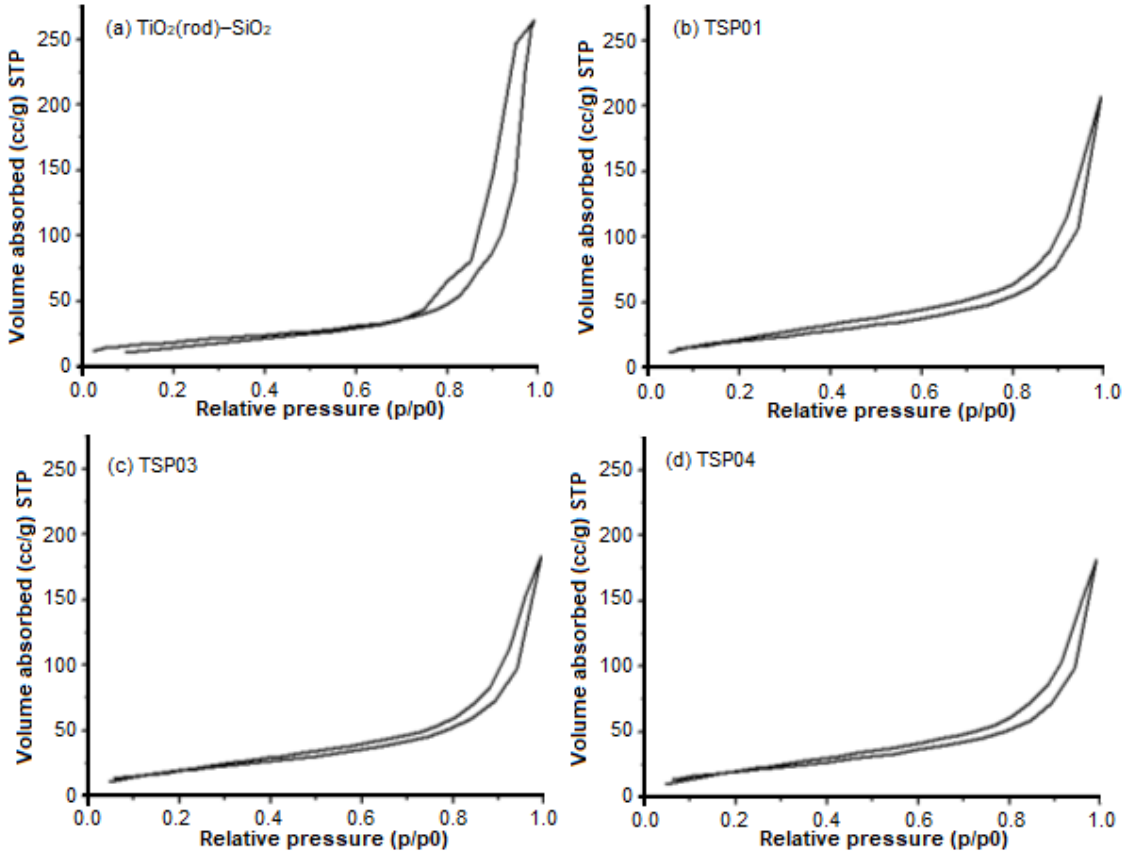

Fig 3. N_2 adsorption-desorption isotherms of the: TiO_2(rod)–SiO_2 (a), and TSP01 (b), TSP-03 (c), and TSP04 (d)

Table 2. The textural properties of TiO_2(rod), TiO_2(rod)–SiO_2, and TSP

Composite	S_{BET} (m^2/g)	V_P (cm^3/g)	D_P (nm)
TiO_2(rod)	63.988	0.344	21.52
TiO_2(rod)–SiO_2	67.561	0.410	24.24
TSP01	77.61	0.320	16.49
TSP03	72.92	0.284	15.58
TSP04	73.82	0.280	15.21

Table 3. The BJH pore size distribution desorption of TiO_2(rod), TiO_2(rod)–SiO_2, and TSP

Composite	S_{BJH} (m^2/g)	V_P (cm^3/g)	D_P (nm)
TiO_2(rod)	71.424	0.349	3.405
TiO_2(rod)–SiO_2	87.352	0.426	9.558
TSP01	71.430	0.307	3.267
TSP03	66.156	0.274	3.291
TSP04	68.505	0.270	3.267

Nitrogen Adsorption-Desorption Isotherm

The nitrogen adsorption-desorption isotherms for TiO_2(rod)–SiO_2 and TSP composites are shown in Fig. 3. The specific surface area was calculated using the standard BET method [25]. The adsorption isotherms of TiO_2(rod)–SiO_2 and TSP (01, 03, and 04) composites are classified as type IV with H1 hysteresis loop in relative pressure of about 0.8. It can be associated with a porous material consisting of well-defined cylindrical-like pore channels [26]. Specific surface area and the other textural parameters are provided in Table 2. The changes in characteristics that include specific area, pore diameter, and pore volume are not too large. These may not affect the photocatalytic performance of the composites significantly.

From BJH pore size distribution desorption data (Table 3), it can be seen that TiO_2(rod)–SiO_2 shows the best character, including of surface area, pore volume and pore diameter. After PANI coating on the TiO_2(rod)–SiO_2 composites, the porosity character decreases. The most striking character decline appears on pore volume and pore diameter of the composites. The decline in porosity character may be due to the thickness of the PANI layer formed so as to cover the active sites on TiO_2(rod)–SiO_2. This decrease in porosity character may affect photocatalytic activity.

TEM Images

The TEM image (Fig. 4a) endorses the formation of TiO_2(rod) with the length size of about 50 nm, and their presence is quite consistent. While TEM image of SiO_2 (Fig. 4b) shows the spherical morphology with the size of about 200 nm, TiO_2(rod) due to the high surface energy tend to be aggregated [5]. The aggregation of TiO_2(rod) was reduced by modifying it with SiO_2 to form TiO_2(rod)-SiO_2. The TEM image of TiO_2(rod)–SiO_2 (Fig. 4c) mixed oxide presents that the core-shell structure did not form completely.

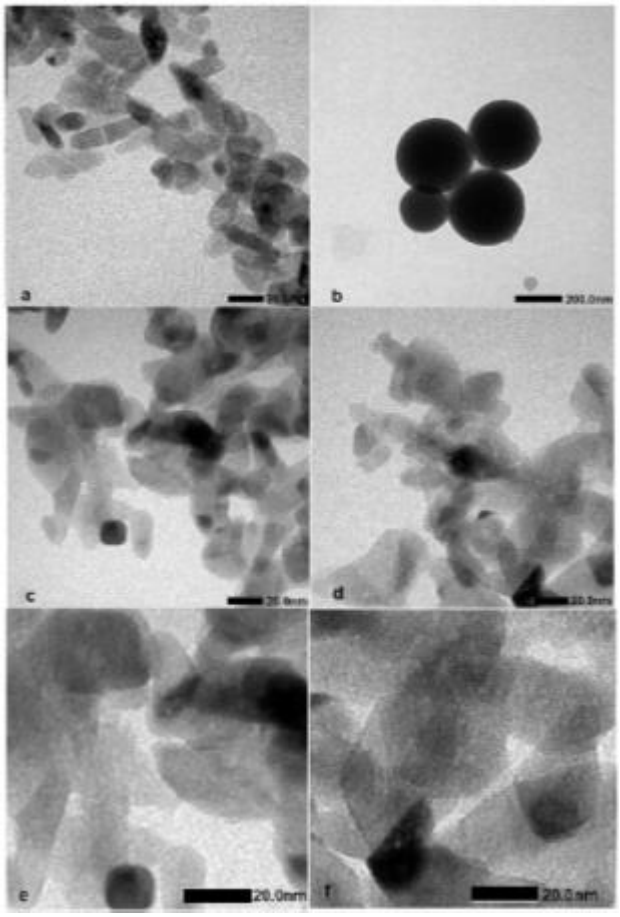

Fig 4. TEM Images of a. TiO_2(rod), b. SiO_2, c & e, TiO_2(rod)-SiO_2, and d & f TSP01

In the TiO_2(rod)–SiO_2 composite, some of the TiO_2(rod) bound on the surface of SiO_2 (dark region) and part of TiO_2(rod) only forms an ordinarily mixed oxide with SiO_2 (Fig. 4e). The composites just arrange

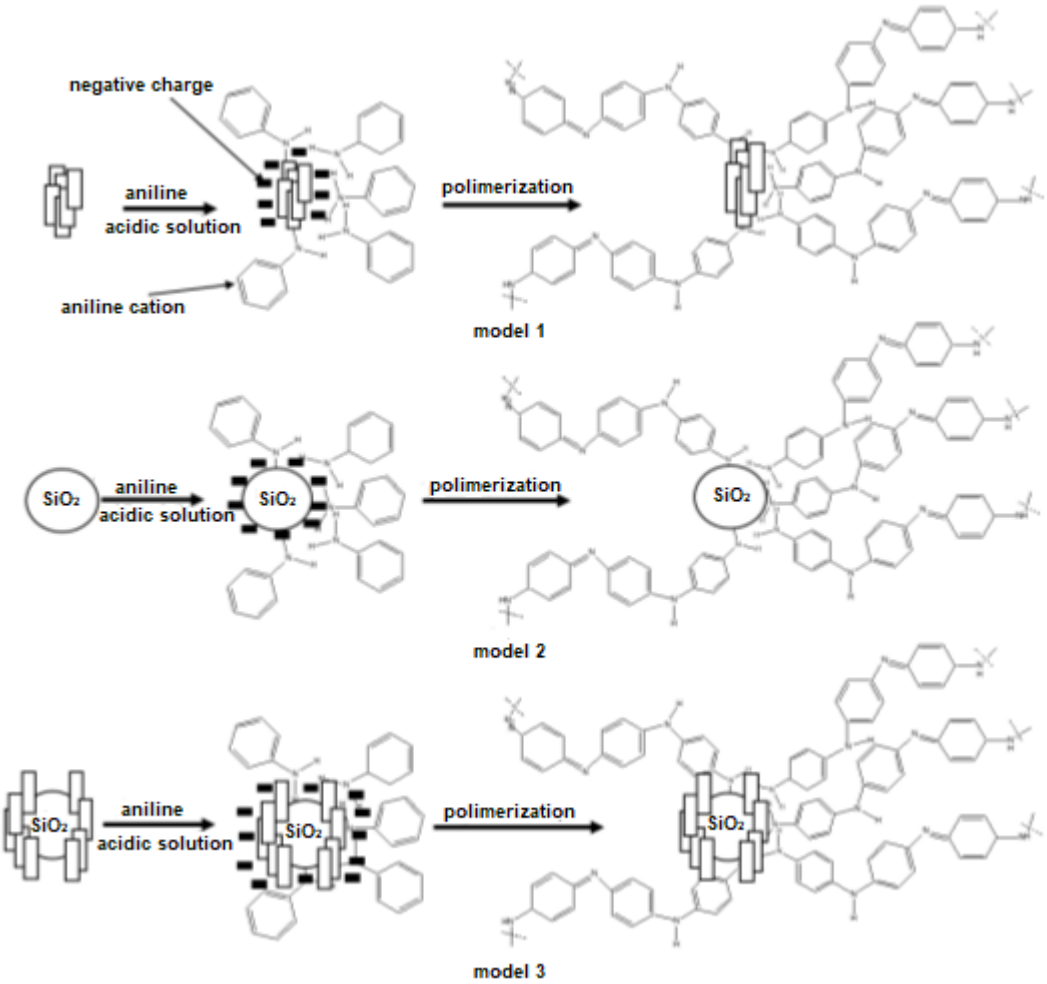

Fig 5. Three models for the polymerization of aniline at the surface of TiO_2(rod), SiO_2, and TSP

as randomly as mixed oxide. The TSP image (Fig. 4d-4f) have wider shape and morphology than TiO_2(rod)–SiO_2, proving that PANI layer has formed around the surface of the mixed oxides. The forming PANI layer in reaction mixture assigned by the green precipitate formation in the suspension.

The Formation of TSP Composites

TiO_2 have isoelectric point at pH = 6 [5]. So, the TiO_2 is positively charged in an acidic solution that is required for the in-situ polymerization of aniline [27]. Fig. 5 illustrated the mechanism of the formation of TSP composite. The surface of TiO_2(rod) is negatively charged due to the adsorbed chloride anions from HCl solution. On the other hand, aniline monomer in acidic solution was transformed to the anilinium cation. Consequently, the electrostatic interaction will occur between negatively charged TiO_2(rod) with anilinium cation. The TEM image (Fig. 4c-4d) did not show the homogeneous formation of the TiO_2(rod)–SiO_2 core-shell structure. It seems that there are TiO_2(rod) and SiO_2 mixed randomly to form a mixed structure.

There is possibility that the covering process of SiO_2 surface by TiO_2(rod) did not work perfectly so several SiO_2 still free as well as several TiO_2(rod). So, there are three possible models (model 1, model 2, and model 3) for the polymerization of aniline on the surface of the composites. Polymerization of aniline may also take place on the surface of TiO_2(rod), on the spherical SiO_2 and on the composite of TiO_2(rod)-SiO_2. SiO_2 such as TiO_2(rod) is also positively charged in acidic solution [13] and Cl^- anion will also be adsorbed on its surface. So, the electrostatic interaction may not only occur on the surface of TiO_2(rod) but also take place on the surface of SiO_2 [28-29]. PANI layers coated on TiO_2(rod) will improve the photosensitization, hence increasing the photocatalytic performance. But, PANI-SiO_2 will not photosensitized TiO_2(rod), thus reducing the photodegradation of the dye pollutant. This mixed structure is predicted to be the cause of the

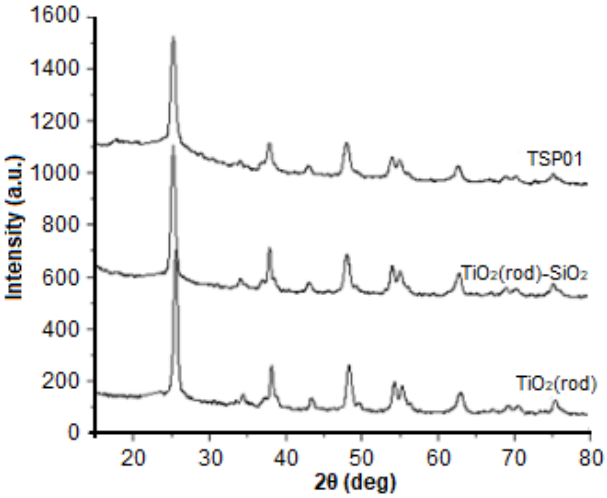

Fig 6. XRD patterns of TiO_2(rod), TiO_2(rod)–SiO_2, and TSP01

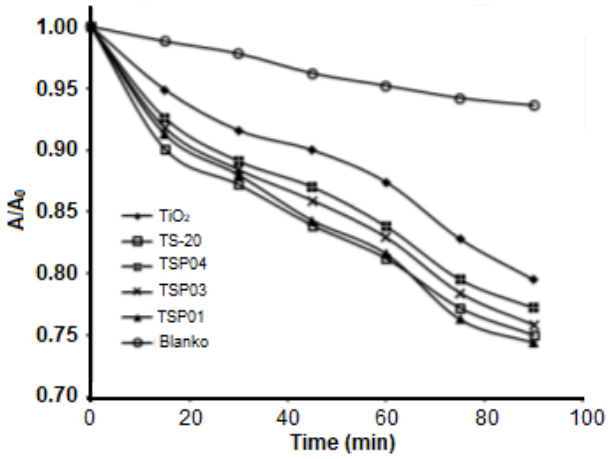

Fig 7. The degradation of methylene blue in TiO_2(rod), TiO_2(rod)-SiO_2, TSP (01, 03, 04), and the blank sample under visible light irradiation

unsignificant improvement of the TSP composites compared to the TiO_2(rod)–SiO_2.

XRD Pattern

XRD patterns of TiO_2(rod), TiO_2(rod)–SiO_2, and TSP composites are illustrated in Fig. 6 The patterns, anatase phase peaks, appeared at 25.19, 37.79 and 47.95, which attributed to the 101, 004, and 200 crystal planes, respectively. This indicated that only anatase phase indexed from the patterns. PANI in the TSP composite particles did not change the peak positions and shapes compared to TiO_2(rod). This showed that the synthesis of TSP did not change the anatase crystalline structure of the TiO_2(rod). The peak intensity of the modified catalyst was lower than the peak of TiO_2(rod). This is evidence that PANI attached on TiO_2(rod). It is also noted that no new diffraction peak appeared in the pattern of TSP composites. This suggests that PANI was not crystalline in the composite structure.

Photocatalytic Activity

Photocatalytic activity investigation was carried out by the degradation of methylene blue in aqueous solution under visible light irradiation. Methylene blue has a maximum absorption at about 663–664 nm. Fig. 7 shows the degradation of methylene blue in aqueous solution in the presence of TiO_2(rod), TiO_2(rod)–SiO_2, and TSP composites with different PANI content and self-degradation of methylene blue under visible light irradiation. The performance of TSP01 and TiO_2(rod)–SiO_2 are better than TiO_2(rod) as indicated by the high percentage of degradation of MB. However, the TSP01 did not show significant improvement of the photocatalytic performance than TiO_2(rod)–SiO_2 composite due to incomplete coverage of PANI layers just on the surface of TiO_2(rod). In addition, the decreasing porosity character that occurs in all TSP composites clearly affects photocatalytic activity. Even porosity in TiO_2(rod)–SiO_2 composites is better than porosity in all TSP composites.

Some PANI layers covered the surface of SiO_2 (shown from the TEM image 6e). TSP03 and TSP04 present a better performance than TiO_2(rod) but lower than the performance of TiO_2(rod)–SiO_2. The lower performance of TSP03 and TSP04 due to the excessive layer of PANI on the surface of mixed oxide which lowering the charge transfer rate. In TSP03 and TSP04, PANI content is about 16.87 and 23.35 wt.%. According to Huang [30], PANI levels that can improve photocatalytic performance in composites (Fe_3O_4/SiO_2/TiO_2/PANI) are about 2.4–4.1 wt.%. Liu et al. [31] found that the content of PANI in the titania fiber-SiO_2 composites that produce the best photocatalytic performance was 2.3 wt.%.

Our study used the aniline of 0.0137–0.0411 M concentration for 5 h polymerization process. A relatively high concentration will result in a thicker PANI layer, especially with relatively long polymerization time. Consequently, if the PANI layer deposited is so thick on the surface of the mixed structure of the mixed oxides, that it will decrease the photocatalytic activity [31]. Liu et al. [31] obtained the best results at low aniline concentrations (0.0109 M) and a short polymerization time of 1 h.

Fig. 8 shows time-dependent UV-Vis spectra of the MB solution in the presence of TSP01. The slight decrease in the absorption peaks of the UV-Vis absorption spectra of MB indicates a slow degradation of MB on the composites. The slow degradation process may also be caused by the low power of the

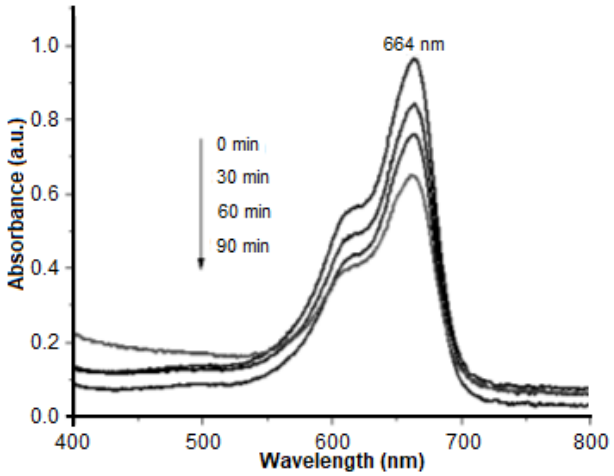

Fig 8. UV-Vis spectra of methylene blue during photocatalytic degradation process under visible light irradiation (TSP01)

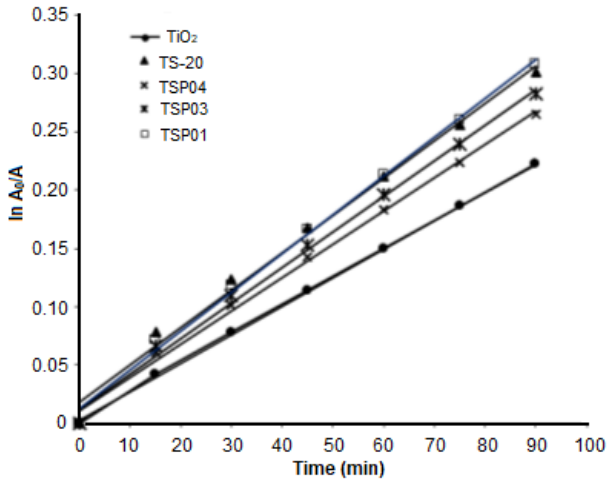

Fig 9. Kinetics plots for the linear fitting of data obtained from pseudo first-order reaction model for methylene blue degradation

Table 3. Apparent rate constants (k_{app}), linear regression coefficients, and degradation efficiency (%) of methylene blue after 90 min irradiation under visible light

Photocatalyst	Degradation efficiency (%) after 90 min	R^2	k_{app} (min^{-1})
TiO_2	20.50	0.984	0.00240
TiO_2-SiO_2	25.03	0.961	0.00296
TSP01	25.59	0.978	0.00315
TSP03	24.18	0.977	0.00288
TSP04	22.84	0.980	0.00272

lamp used in our study of 100 W. Some researchers use 500 W Xenon or Mercury lamps [31-33].

Similar percentage of MB degradation has also been achieved by Huang et al. [30]. It was found that PANI layer of about 2.4 wt.% on the $Fe_3O_4/SiO_2/TiO_2$ surface provides the best performance of reducing MB concentration of about 35% for 300 min 300 W visible light irradiation. In our study the lowest PANI content was about 9.2 wt.% on the surface of TiO_2(rod)–SiO_2 (TSP01). Therefore, there is a big possibility of slowing down the charge transfer rate on the composite surface, hence the improved photocatalytic performance is not significant. However, the photocatalytic performance of about 25% using only 100 W Xenon lamps can be achieved using shorter irradiation time compare to Huang et al., [30]. This may be ascribed to the use of the nanorod structure of TiO_2 [17].

The kinetics plots for methylene blue degradation with those composites are shown by apparent first order reaction [34-35] in Fig. 9. This model is described by the equation: $-\ln (A_t/A_o) = k_{app}\, t$, where k_{app} is the apparent rate constant, A_o is the initial absorbance of methylene blue and A_t is the absorbance of methylene blue at a various contact time, t. The activity of TiO_2(rod), TiO_2(rod)–SiO_2, and TSP composites can be evaluated by comparing the value of k_{app} listed in Table 3.

The TSP composites with various PANI content show comparable photocatalytic activity to the TiO_2(rod)–SiO_2. The inclusion of PANI into the TiO_2(rod)–SiO_2 system with the relatively high content of PANI (TSP03 and TSP04) decreases the rate of methylene blue degradation reaction. The decrease in the reaction rate at a relatively high PANI level may be due to the excessive layer of PANI covering the active site of TiO_2(rod)–SiO_2, then lowering the charge transfer rate [32]. This may also be due to the presence of a mixed structure of TiO_2(rod)–SiO_2 that tend to form a mixed oxide than the core-shell structure so some of PANI coated on the SiO_2 rather than TiO_2(rod). The apparent rate constants, regression coefficients, and degradation efficiency of methylene blue are tabulated in Table 3. The regression coefficients obtained in this research follow the apparent first order reaction kinetics.

CONCLUSION

TiO_2 with rod-like shape were mixed with SiO_2 spherical to become TiO_2(rod)–SiO_2 composite resulting in a mixed structure of the oxides and composites, that is TiO_2(rod)–SiO_2, TiO_2(rod), and SiO_2. Aniline forms PANI on the surface of all mixed

structures of the oxides and the composites, TiO_2(rod), SiO_2, and TiO_2(rod)-SiO_2. The TSP (TiO_2(rod)–SiO_2-PANI) composites with various PANI content show the photocatalytic activity as well as T TiO_2(rod)–SiO_2 but the performance did not improve significantly. The low percentage of MB degradation is maybe caused by the excessive layer of PANI on the TiO_2(rod)–SiO_2 composite as well as the formation of mixed structures.

REFERENCES

[1] Wang, D.P., and Zeng, H.C., 2009, Multifunctional roles of TiO_2 nanoparticles for architecture of complex core-shells and hollow spheres of SiO_2-TiO_2-polyaniline system, *Chem. Mater.*, 21 (20), 4811–4823.

[2] Xiong, S., Phua, S.L., Dunn, B.S., Ma, J., and Lu, X., 2010, Covalently bonded polyaniline-TiO_2 hybrids: A facile approach to highly stable anodic electrochromic materials with low oxidation potentials, *Chem. Mater.*, 22 (1), 255–260.

[3] Watoni, A.H., Gandasasmita, S., and Noviandri, I., 2007, Electrochemical synthesis and characterization of polypyrrole for electrochemical synthezis dodecylsulfate sensor membrane, *Indones. J. Chem.*, 7 (3), 249–253.

[4] Li, X., Wang, D., Cheng, G., Luo, Q., An, J., and Wang, Y., 2008, Preparation of polyaniline-modified TiO_2 nanoparticles and their photocatalytic activity under visible light illumination, *Appl. Catal., B*, 81 (3-4), 267–273.

[5] Olad, A., Behboudi, S., and Entezami, A.A., 2012, Preparation, characterization and photocatalytic activity of TiO_2/polyaniline core-shell nanocomposite, *Bull. Mater. Sci.*, 35 (5), 801–809.

[6] Li, J., Zhu, L., Wu, Y., Harima, Y., Zhang, A., and Tang, H., 2006, Hybrid composites of conductive polyaniline and nanocrystalline titanium oxide prepared via self-assembling and graft polymerization, *Polymer*, 47, 7361–7367.

[7] Wang, L.Y., Sun, Y.P., and Xu, B.S., 2008, Comparison study on the size and phase control of nanocrystalline TiO_2 in three Ti–Si oxide structures, *J. Mater. Sci.*, 43 (6), 1979–1986.

[8] Sirimahachai, U., Ndiege, N., Chandrasekharan, R., Wongnawa, S., and Shannon, M.A., 2010, Nanosized TiO_2 particles decorated on SiO_2 spheres (TiO_2/SiO_2): Synthesis and photocatalytic activities, *J. Sol-Gel Sci. Technol.*, 56 (1), 53–60.

[9] Iengo, P., Di Serio, M., Sorrentino, A., Solinas, V., and Santacesaria, E., 1998, Preparation and properties of new acid catalysts obtained by grafting alkoxides and derivatives on the most common supports note I — grafting aluminium and zirconium alkoxides and related sulphates on silica, *Appl. Catal., A*, 167 (1), 85–101.

[10] Gao, X., and Wachs, I.E., 1999, Titania–silica as catalysts: Molecular structural characteristics and physico-chemical properties, *Catal. Today*, 51 (2), 233–254.

[11] Zhang, M., Shi, L., Yuan, S., Zhao, Y., and Fang, J., 2009, Synthesis and photocatalytic properties of highly stable and neutral TiO_2/SiO_2 hydrosol, *J. Colloid Interface Sci*., 330 (1), 113–118.

[12] Smitha, V.S., Manjumol, K.A., Baiju, K.V., Ghosh, S., Perumal, P., and Warrier, K.G.K., 2010, Sol-gel route to synthesize titania-silica nano precursors for photoactive particulates and coatings, *J. Sol-Gel Sci*. *Technol.*, 54 (2), 203–211.

[13] Wilhelm, P., and Stephan, D., 2006, On-line tracking of the coating of nanoscaled silica with titania nanoparticles via zeta-potential measurements, *J. Colloid Interface Sci*., 293 (1), 88–92.

[14] Suprabha, T., Roy, H.G., Thomas, J., Kumar, K.P., and Mathew, S., 2008, Microwave-assisted synthesis of titania nanocubes, nanospheres and nanorods for photocatalytic dye degradation, *Nanoscale Res. Lett.*, 4 (2), 144–152.

[15] Zhang, H., Liu, P., Liu, X., Zhang, S., Yao, X., An, T., Amal, R., and Zhao, H., 2010, Fabrication of highly ordered TiO_2 nanorod/nanotube adjacent arrays for photoelectrochemical applications, *Langmuir*, 26 (13), 11226–11232.

[16] Kumar, A., Madaria, A.R., and Zhou, C., 2010, Growth of aligned single-crystalline rutile TiO_2 nanowires on arbitrary substrates and their application in dye-sensitized solar cells, *J. Phys. Chem. C*, 114 (17), 7787–7792.

[17] Yun, H.J., Lee, H., Joo, J.B., Kim, W., and Yi, J., 2009, Influence of aspect ratio of TiO_2 nanorods on the photocatalytic decomposition of formic acid, *J. Phys. Chem. C*, 113 (8), 3050–3055.

[18] Wahyuni, S., Kunarti, E.S., Swasono, R.T., and Kartini, I., 2017, Study on the properties and photoactivity of TiO_2(nanorod)–SiO_2 synthesized by sonication technique, *Orient. J. Chem.*, 33 (1), 249–257.

[19] Song, L., Qiu, R., Mo, Y., Zhang, D., Wei, H., and Xiong, Y., 2007, Photodegradation of phenol in a polymer-modified TiO_2 semiconductor particulate system under the irradiation of visible light, *Catal. Commun.*, 8 (3), 429–433.

[20] Zhu, Y., Xu, S., and Yi, D., 2010, Photocatalytic degradation of methyl orange using polythiophene/titanium dioxide composites, *React. Funct. Polym*., 70 (5), 282–287.

[21] Zhang, L., Liu, P., and Su, Z., 2006, Preparation of PANI-TiO_2 nanocomposites and their solid-phase

photocatalytic degradation, *Polym. Degrad. Stab*., 91 (9), 2213–2219.

[22] Irmak, S., Kusvuran, E., and Erbatur, O., 2004, Degradation of 4-chloro-2-methylphenol in aqueous solution by UV irradiation in the presence of titanium dioxide, *Appl. Catal., B*, 54 (2), 85–91.

[23] Sato, T., Masaki, K., Sato, K., Fujishiro, Y., and Okuwaki, A., 1996, Photocatalytic properties of layered hydrous titanium oxide/CdS-ZnS nanocomposites incorporating CdS-ZnS into the interlayer, *J. Chem. Technol. Biotechnol.*, 67 (4), 339–344.

[24] Hsien, Y., Chang, C., Chen, Y., and Cheng, S., 2001, Photodegradation of aromatic pollutants in water over TiO_2 supported on molecular sieves, *Appl. Catal., B*, 31 (4), 241–249.

[25] Brunauer, S., Emmett, P.H., and Teller, E., 1938, Adsorption of gases in multimolecular layers, *J. Am. Chem. Soc.*, 60 (2), 309–319.

[26] Carja, G., Nakamura, R., Aida, T., and Niiyama, H., 2001, Textural properties of layered double hydroxides: Effect of magnesium substitution by copper or iron, *Microporous Mesoporous Mater*., 47(2-3), 275–284.

[27] Salem, M.A., Al-Ghonemiy, A.F., and Zaki, A.B., 2009, Photocatalytic degradation of Allura red and Quinoline yellow with polyaniline/TiO_2 nanocomposite, *Appl. Catal., B*, 91 (1-2), 59–66.

[28] Wang, T.T., Liu, X.H., Guo, J.J., Cheng, Y.C., Xu, G.J., and Cui, P., 2013, Synthesis and electrorheological properties of SiO_2/polyaniline nanocomposites prepared by *in-situ* polymerization, *Adv. Mater. Res.*, 669, 131–137.

[29] Zengin, H., and Erkan, B., 2010, Synthesis and characterization of polyaniline/silicon dioxide composites and preparation of conductive films, *Polym. Adv. Technol*., 21 (3), 216–223.

[30] Huang, X., Wang, G., Yang, M., Guo, W., and Gao, H., 2011, Synthesis of polyaniline-modified $Fe_3O_4/SiO_2/TiO_2$ composite microspheres and their photocatalytic application, *Mater. Lett.*, 65 (19-20), 2887–2890.

[31] Liu, Z., Miao, Y.E., Liu, M., Ding, Q., Tjiu, W.W., Cui, X., and Liu, T., 2014, Flexible polyaniline-coated TiO_2/SiO_2 nanofiber membranes with enhanced visible-light photocatalytic degradation performance, *J. Colloid Interface Sci*., 424, 49–55.

[32] Li, X., Wang, D., Luo, Q., An, J., Wang, Y., and Cheng, G., 2008, Surface modification of titanium dioxide nanoparticles by polyaniline via an *in situ* method, *J. Chem. Technol. Biotechnol*., 83 (11), 1558–1564.

[33] Zhang, H., Zong, R., Zhao, J., and Zhu, Y., 2008, Dramatic visible photocatalytic degradation performances due to synergetic effect of TiO_2 with PANI, *Environ. Sci. Technol*., 42 (10), 3803–3807.

[34] Li, X., Teng, W., Zhao, Q., and Wang, L., 2011, Efficient visible light-induced photoelectrocatalytic degradation of rhodamine B by polyaniline-sensitized TiO_2 nanotube arrays, *J. Nanopart. Res.*, 13 (12), 6813–6820.

[35] Wang, F., Min, S., Han, Y., and Feng, L., 2010, Visible-light-induced photocatalytic degradation of methylene blue with polyaniline-sensitized TiO_2 composite photocatalysts, *Superlattices Microstruc.*, 48 (2), 170–180.